Proceedings of the ASME 2020 International Technical Conference and Exhibition
on Packaging and Integration of Electronic and Photonic Microsystems
InterPACK2020
October 27-29, 2020, Virtual, Online

IPACK2020-2592

CFD ANALYSIS ON LIQUID COOLED COLD PLATE USING COPPER NANOPARTICLES

Pardeep Shahi[1], Sarthak Agarwal, Satyam Saini, Amirreza Niazmand, Pratik Bansode, Dereje Agonafer
The University of Texas at Arlington
Arlington, TX

ABSTRACT

In today's world, most data centers have multiple racks with numerous servers in each of them. The high amount of heat dissipation has become the largest server-level cooling problem for the data centers. The higher dissipation required, the higher is the total energy required to run the data center. Although still the most widely used cooling methodology, air cooling has reached its cooling capabilities especially for High-Performance Computing data centers. Liquid-cooled servers have several advantages over their air-cooled counterparts, primarily of which are high thermal mass, lower maintenance. Nano-fluids have been used in the past for improving the thermal efficiency of traditional dielectric coolants in the power electronics and automotive industry. Nanofluids have shown great promise in improving the convective heat transfer properties of the coolants due to a proven increase in thermal conductivity and specific heat capacity.

The present research investigates the thermal enhancement of the performance of de-ionized water-based dielectric coolant with Copper nanoparticles for a higher heat transfer from the server cold plates. Detailed 3-D modeling of a commercial cold plate is completed and the CFD analysis is done in a commercially available CFD code ANSYS CFX. The obtained results compare the improvement in heat transfer due to improvement in coolant properties with data available in the literature.

Keywords: CFD, particle transport, data center, contamination.

[1] Contact author: pardeep.shahi@mavs.uta.edu

NOMENCLATURE

C_P	Specific heat capacity (kJ. /kg-K)
k	Thermal conductivity (W/mK)
P	Pressure (Pa)
$MCHS$	Micro-Channel Heat Sibk
Δp	Pressure drop (Pa)
Q	Interphase heat transfer (W)
T	Temperature (°C)
Re	Reynolds Number

Greek Symbols

Φ	Volume fraction / Nanofluid Concentration
μ	Viscosity (kg/m.s)
ρ	Density (kg/m^3)

Subscripts

f	Fluid
nf	Nanofluid
s	Solid particle
w	Wall

INTRODUCTION

A gradual and consistent increase in data processing demands has boosted the server power consumption for modern-day data centers. Statistics in the literature suggest that approximately 2% of the entire power consumption in the United States in 2010 was by data centers. This percentage increased by 8.7% over the years 2011 and 2012 and was expected to increase by 9.8% over the following year. A major portion of this power in a typical data center, almost 40%, is attributed to the electricity utilization by the cooling systems [1]. Therefore, energy-efficient and cost-effective solutions that reduce the cooling requirements, maintaining efficient and reliable device operation, are vital at the chip, server, and rack-level.

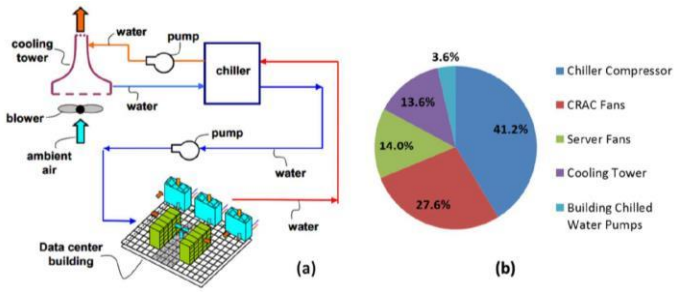

FIGURE 1: (a) TRADITIONAL AIR COOLED DATA CENTER COOLING INFRASTRUCTURE (b) ENERGY BREAKDOWN FOR AN AIR-COOLED DATA CENTER

The size of a data center white space depends on various factors such as the number and size of the racks for servers and the area required for power distribution and cooling equipment. For high-performance computing, a significant amount of heat flux needs to be dissipated from each of the processing units for continuous reliable operation of the servers and minimal downtime. The conventional and the most widely used type of cooling used today is air cooling where cold air is forced through the channels of the heat sinks mounted on the primary heat-dissipating chips for a higher heat transfer [2]. The main advantages of the air-cooling are that most of the fans do not require a lot of power as compared to the power consumed by a combination of pumps in liquid cooling, which in turn benefits the operational costs, initial setup costs. It has an easier assembly than the liquid-cooled systems and no concern of damage from fluid leakage on the printed circuit boards (PCB). In the recent past, immersion cooling has become another popular way for cooling high heat-dissipating information and technology (IT) equipment where a dielectric fluid comes in direct contact with the complete PCB that is submerged in a tank. This process of direct contact heat dissipation can be accompanied by a phase change of the coolant in two-phase immersion type cooling where the latent heat of low boiling point fluorocarbons is used for cooling of hot surfaces on the PCB. While immersion cooling technologies are known to provide power usage effectiveness (PUE) of less than 1.1, the reliability and serviceability concerns still need to be addressed for implementation at larger scales.

Liquid cooling is generally a closed-loop system that has a coolant running through the manifold, pumped within the servers through the cold plates using either a centralized or a distributed pumping system. This conjugate heat transfer approach for cooling of servers dissipates heat using a copper cooling plate with micro-channels mounted on top of the processor, through which the coolant passes. Thermal Interface Material (TIM) is usually placed between the copper plate and the processor to maintain the thermal coupling and minimize contact related thermal losses. This approach offers an effective passage to transfer heat as compared to conventional mechanical air cooling techniques that utilizes CRAC units supplying redundant airflow while consuming a large amount of energy as well. An in-depth account of various cooling methods implemented from handheld devices to datacenters has been discussed in the literature [3–5]. It was reported by Ellsworth and Iyengar [6] that by implementing a hybrid cooling system using both air and water, approximately, a 45% of reduction in the facility power consumption was achievable as compared to a fully air cooling-based system. The energy savings can further be augmented by 50% when all of the heat dissipated is transported directly to chilled water in the racks. David et al. [7] showed that an energy savings of about 25% can be attained by adopting a chiller less data center facility with higher coolant inlet and recirculated air-cooled servers. Also, data center space saving sof almost 30-40% have been reported by resorting to liquid 30–40% [8].

In liquid cooling systems, different types of coolants can be used based on heat transfer requirements and pressure drop limitations. These coolants, for example, maybe water & ethylene glycol-based mixtures, metal oxide nanoparticle-based liquid coolant mixtures, etc. This research work aims to improve the thermal performance of an existing cold plate design using copper oxide-based nanofluid using CFD. For the present investigation, a de-ionized water-based copper oxide nanofluid was taken into consideration for heat transfer enhancement for a micro-channel cold plate. A base case was used for validation of the results by comparing the results obtained to that in the recently published literature for a cold plate of a similar design and flow parameters [8]. The concentration and inlet temperature of the nanofluid mixture was varied to judge the improvement in the heat transfer characteristics. The difference in temperature at the cold plate, pressure drop across the cold plate, and the outlet temperatures are measured and superimposed with the validation data to get an exact idea of the thermal performance enhancement achieved.

LITERATURE REVIEW

Researchers and engineers have been introducing various techniques for heat transfer enhancement since the 1950s. Among the many of these published research works, several popular review articles [9-11] and handbook chapters [12-14], discussing a range of techniques for enhancing heat transfer, are available in the reviewed literature. To begin with, nanofluids were used in transformers in conjunction with mineral oil as well as heat exchangers to improve heat removal. Over the past three decades, there has been a lot of research interest, both for experimental and numerical investigations, due to the breakthrough work by Tuckerman and Pease [15,16]. They characterized thermal capabilities of the microchannel heat sinks (MCHS) in dissipating large amounts of heat fluxes. A MCHS is typically characterized by a large number of parallel microchannels. The hydraulic diameter for typical MCHSs generally lies between a range of 10 to 1000 μm where the cooling fluid passes through these channels carrying away the heat from a hot surface, which is generally below the heat sink. Empiriacal literature shows that MCHSs have several unique characyeristics as compared to conventional air cooled heat removal devices, for example, higher heat transfer coefficient, smaller area and volume per heat load, lower coolant volume

requirement, etc. [17,18]. Other than the experimental literature, heat transfer calculations, and optimization of the MCHS geometry based on theoretical results and numerical analysis have been carried out in past research as well [19,20]. As per the reviewed literature, air, water and fluoro-chemicals are the most widely used coolants for studying MCHSs. But the heat transfer capabilities of these fluids are usually limited by their thermos-physical properties. An enhancement in these properties can be achieved by adding additives to the working fluid that improves the thermal transport properties and flow parameters [21,22]. This enhancement in the heat transfer properties has been achieved by experimental and analytical studies in past. These investigations showed that using nanofluids, higher thermal conductivities are posbile as compared to pure fluids. Therefore, these enhanced fluids are a viable option for improved heat transfer with the nano particle being either metallic or non-metallic, based on the application.

Theoretical models for prediction of heat transfer characteristics were proposed by Xuan and Roetzel for tube flow containing nanoparticles [27]. Experimental measurements for convective heat transfer and pressure drop were carried out [28-30] which concluded that the heat transfer coefficient was significantly improved and its value was dependent on the flow Reynolds number, particle Peclet number, the particle physical properties like volume fraction fraction, size and shape. Their results also showed that nanoparticles did not cause a dramatic rise in the pressure drop. An experimental study carried out by Yang et al. [31] aimed to formulate a heat transfer correlation among various parameters that affect the rate of heat transfer. The study showed that, for a circular duct flow, there was not an appreciable improvement in the heat transfer coefficient for a laminar flow regime for a laminar flow regime using the conventional heat transfer for base as well as the particle laden fluid. Theorectical assessment and development of macroscale correlations for heat transfer improvement using nanofluids in MCHSs [32,33]

NUMERICAL ANALYSIS

3.1 Conservation Equations

The CFD solver used in this study, ANSYS CFX, solves instantaneous equations of mass, momentum, and energy conservation to resolve laminar flows and are given by equations (1), (2) and (3) respectively [34]. As the flow for present investigation is laminar, extra closure or time-averaged equation models are not activated in the solver which also reduced simulation time.

Continuity equation

$$\frac{\partial \rho}{\partial_t} + \nabla \cdot (\rho U) = 0 \tag{1}$$

Momentum Equation

$$\frac{\partial}{\partial t}(\rho U) + \nabla \cdot (\rho U U) = -\nabla_P + \nabla_\tau + S_M \tag{2}$$

Total Energy equation

$$\frac{\partial(\rho h_{tot})}{\partial t} - \frac{\partial p}{\partial t} + \nabla \cdot (\rho \boldsymbol{U} h_{tot}) = \nabla \cdot (\lambda \nabla T) + \nabla \cdot (\boldsymbol{U} \cdot \tau) + \boldsymbol{U} \cdot \boldsymbol{S_M} + \boldsymbol{S_E} \tag{3}$$

3.2 Basic assumptions applied to the simulation

Particle forces and particle physical properties of size and shape were ignored for the present simulation. The flow considered did not include and compressibility or transient effects. As the geometry is very small, the effects of gravity are ignored in the direction transverse to the flow. Temperature dependednt properties were not considered for the simulations and the effect of viscous heating and radiative heat transfer are ignored.

3.3 Nanofluid Thermo-physical Properties

The thermos-physical properties of the nanofluid were calculated theoretically by referring to various popular models available in the literature. These models assume that particles are solids suspended in a pure fluid and the presence of these particles alter or enhance the properties of the base pure fluid. The most important properties that affect the convective heat transfer phenomenon are viscosity, thermal conductivity, specific heat capacity, and density of the fluid or coolant and are directly proportional to the volume fraction of the suspended particles. The decisive factors in determining the enhancement in convective heat transfer in nanofluids. Equation 7 proposed by Purohit et al [35] was used to calculate the thermal conductivity for the present investigation. The effect of particle shape and size is neglected in all of the equations considered for this study. To determine the change in specific heat, density and, viscosity equations proposed by Das et al [36], Wang et al [37] and, Brinkman et al [38] were reviewed and are given below:

Density

$$(\rho_{nf}) = (1-\phi)_{\rho_f} + \phi \rho_s \tag{4}$$

Specific Heat

$$(\rho c_p) nf = (1-\phi)(\rho Cp)_f + \phi(\rho Cp)p \tag{5}$$

Viscosity

$$\mu_{nf} = \mu_f (1-\phi)^{-2\cdot 5} \tag{6}$$

Thermal Conductivity

$$k_{nf} = k_f \left[\frac{k_s + 2k_f + 2\phi(k_f - k_s)}{k_s + 2k_f - \phi(k_f - ks)}\right] \tag{7}$$

GEOMETRY, MESH, AND BOUNDARY CONDITIONS

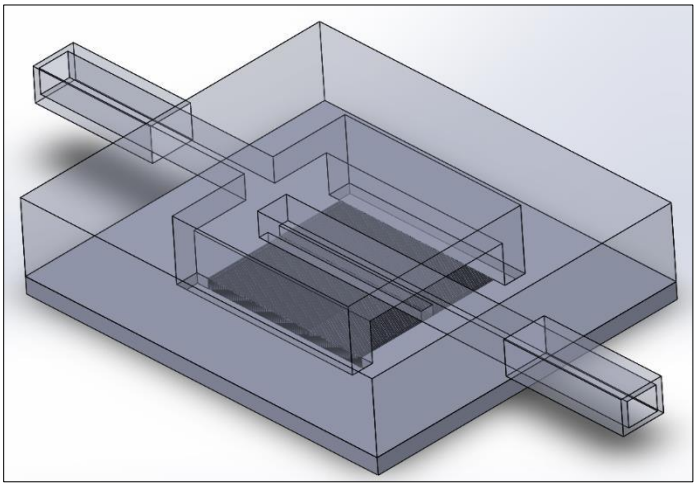

FIGURE 2: DETAILED CAD MODEL COLD PLATE GEOMETRY

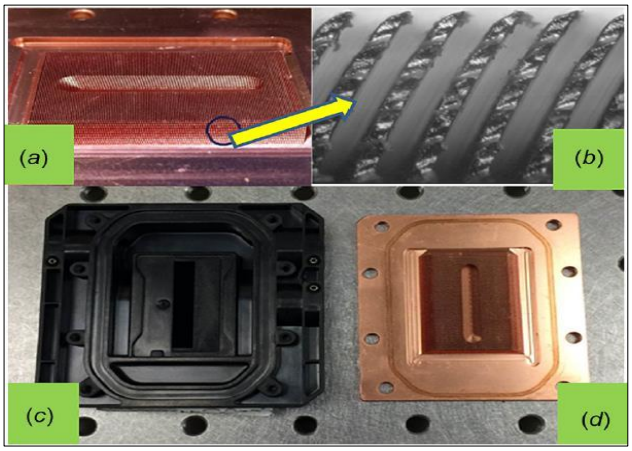

FIGURE 3: CooLIT COLD PLATE [49]

The detailed 3D modeling of the cold plate was done using SolidWorks as shown in Figure 2. The complete assembly of the cold plate includes the copper plate (grey), the top cover (transparent), and the fluid domain. A boundary condition of uniform heat flux source was defined at the bottom of the copper plate, depicting a processor. The coolant flow velocity and temperature were specified at the inlet and a 0 Pa static pressure condition was defined at the outlet. The surfaces of the top cover were assumed to be adiabatic. The dimensions of the fins and channels were the same as the experimental setup used by Ramakrishnan et al [8] and are given in Table 2. The design of the cold plate geometry and the dimensions were modeled as per a commercially available cold plate by CoolIT as shown in Figure 3. 3(b) shows a zoomed-in view of the microchannels, 3(c) shows the non-conductive top plate of the cold plate, while 3(d) shows the copper plate with microchannels.

Particle Volume Fraction (%)	Density (kg/m^3)	Specific Heat (J/kgK)	Thermal Conductivity (w/mK)	Viscosity (kg/ms)
0.2	998.2	4165	0.61	8.92e-04
0.3	1237.6	4161	0.62	8.94e-04
0.4	1397.2	4157	0.65	8.99e-4

TABLE 1: CALCULATED PROPERTIES OF THE FLUID USED FOR SIMULATIONS [15]

Cold plate dimensions	
Length of channel	31.52mm
Breath of channel	23.56mm
Thickness of fin	100.6 μm
Channel width	154.3 μm
Height of fin	2.02mm
Thickness of base	1.35mm

TABLE 2: COLD PLATE DIMENSIONS

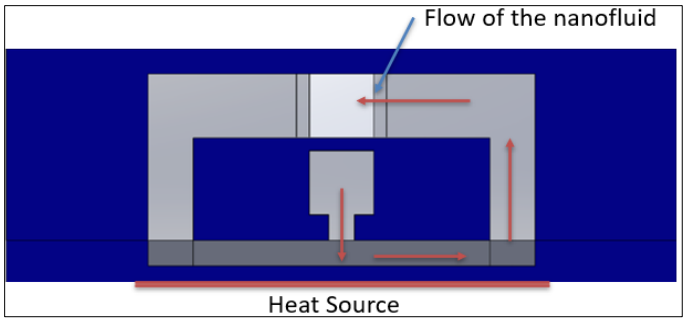

FIGURE 4: CROSS SECTION ILLUSTRATING THE FLOW DIRECTION AND HEAT SOURCE

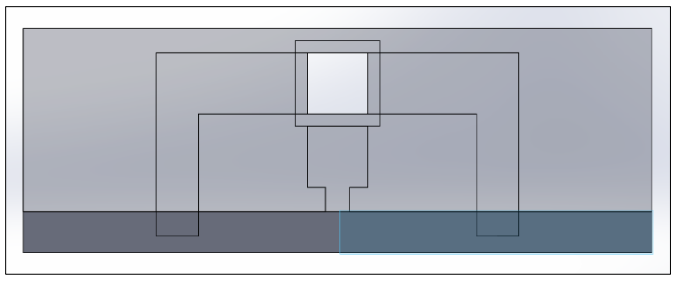

FIGURE 5: FRONT SECTION VIEW

The heat source is located at the bottom of the cold plate highlighted in red in Figure 4, where a constant heat flux boundary condition was given. The heat source was modeled after an actual processor's dimensions. The bottom plate is made

from pure copper and the top transparent portion of the plate is made from a non-conducting material such as plastic or rubber. Figure 5 illustrates the sectional front view of the geometry. The coolant flows into the bottom copper plate into the center grove and distributes in the channels and leaves to the outlet at the end of the channel. It was, thus, concluded by the authors that simulating the flow in complete geometry would lead to excessively high number of elements for a good quality mesh. Therefore, only one half of a single channel with a periodic boundary condition was simulated to represent the flow in the entire geometry. This enabled the authors to create a dense mesh at the area of interest, i.e. one microchannel with an extremely dense mesh of approximately 1.08 million, all hexahedral elements using ICEM CFD as shown in Figure 6.

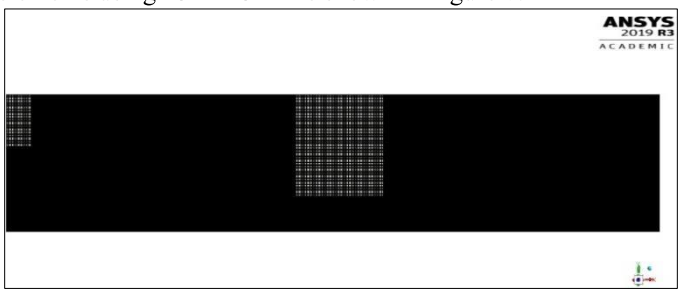

FIGURE 6: DENSE MESH AT MICROCHANNEL

Number of Elements (x 10^6)	Source Temperature (°C)
0.3	30
0.8	27
1.1	26.8
1.5	26.5

TABLE 3: RESULTS FOR GRID INDEPENDENCE

As mentioned earlier, mesh density governs the accuracy of the results which is why it was vital to have sufficiently a high number of elements in the flow domain, especially near the walls to capture the near wall boundary layer effects. A mesh sensitivity analysis provided the appropriate number of elements to be used for accurate results, as shown in table 3. Figure 7 represents the. The validation results for the entire cold plate were also compared with the case of a single fin and a close agreement was obtained, implying that the meshing parameters for a single channel were correctly assigned.

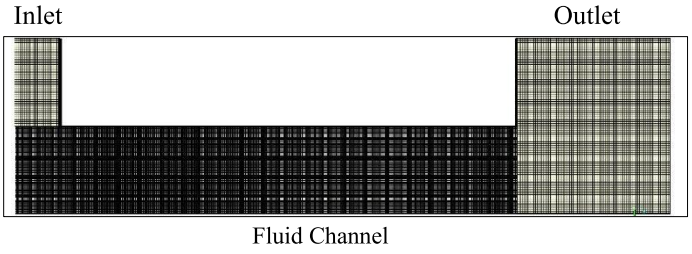

FIGURE 7: MESH OF THE FLUID DOMAIN

RESULTS AND DISCUSSIONS

A total of 27 simulations were completed for varying inlet temperatures, flow rate and nanofluid concentration as shown in Table 4. To validate the results obtained from the CFD using the specified boundary conditions, experimental results obtained for the same cold plate by Ramakrishnan et al [8] were referred. Figure 8 shows the comparison of coolant outlet temperatures for varying power at heat source v/s the flow rate. The validation was carried out for 4 different power values of 100W, 125W, 175W and 210W, and at 6cm^3/s and 13 cm^3/s inlet volumetric flow rates. A maximum temperature difference of approximately 0.5°C was obtained for all the input power values between the two studies.

S.No	Flow rate (cm^3/s)	Inlet Temperature	Concentration (%)
1	1	25	0.2
2	3	35	0.3
3	6	45	0.4

TABLE 4: LIST OF PARAMETERS VARIED FOR SIMULATIONS

As a good agreement was obtained between the results, these were considered as baseline values for comparison with results obtained after using enhanced nanofluid properties. Figure 10 shows the variation of maximum CPU temperature with change in nanoparticle concentration in the base fluid. To assess the heat transfer improvement obtained by adding nanoparticles to the base fluid, deionized water in this case, the dimensionless flow parameters like Nusslet Number, Prandtl Number and improvement in the value of the convective heat transfer coefficient was analyzed.

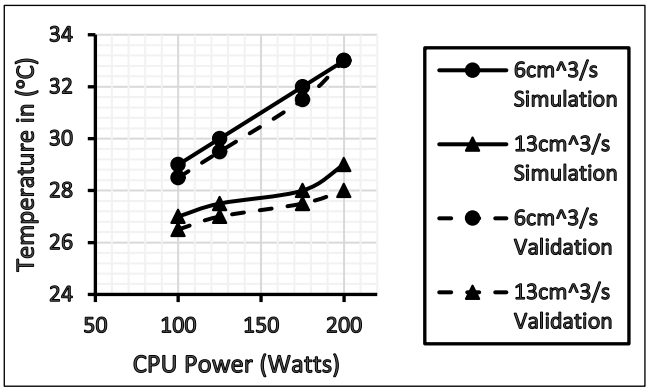

FIGURE 8: RESULT FOR TEMPERATURE VALIDATION [8]

Thermal conductivity is the factor due to which there is heat transfer from the walls to the liquid whereas the specific heat capacity is the parameter which enables the fluid to carry the heat. When the nanoparticle concentration in the fluid increases, the thermal conductivity of the nanofluid is increased but the heat capacity is reduced by some margin. The reduction in the heat capacity varies with the type of model used for calculating the nanofluid properties. Therefore, there might be an optimum value of the volume fraction of the nanoparticles that can be

added to achieve maximum convective heat transfer enhancement and minimum pressure drop penalty. For the current set of simulations, a total pressure difference of approximately 10 Pa was observed across the channel as shown in Figure 9. The reviewed literature also suggests that the pressure drop variation is generally not very significant but may increase depending on the nature of the geometry due to localized perturbations in the flow.

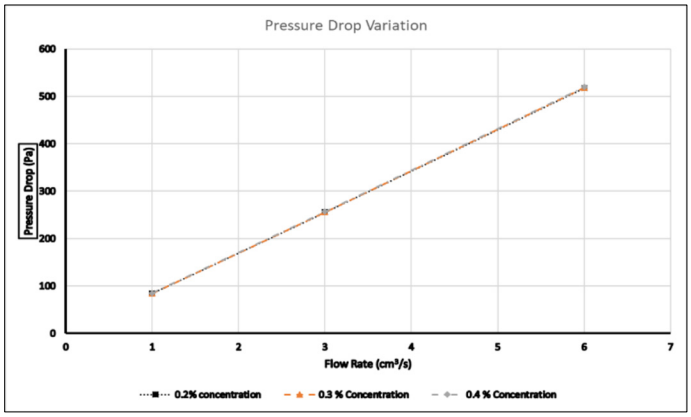

FIGURE 9: EFFECT OF VOLUMETRIC CONCENTRATION OF NANOPARTICLES ON CHANNEL PRESSURE DROP FOR VARYING FLOW RATES

The variation of CPU temperature with varying inlet temperatures for different particle concentrations can be seen in Figure 10. A maximum temperature difference of 0.5°C was observed for the for the case of minimum flow rate considered. While this might seem not a significant temperature reduction, it is not a true measure of heat transfer improvement within the system as will be discussed later in this section.

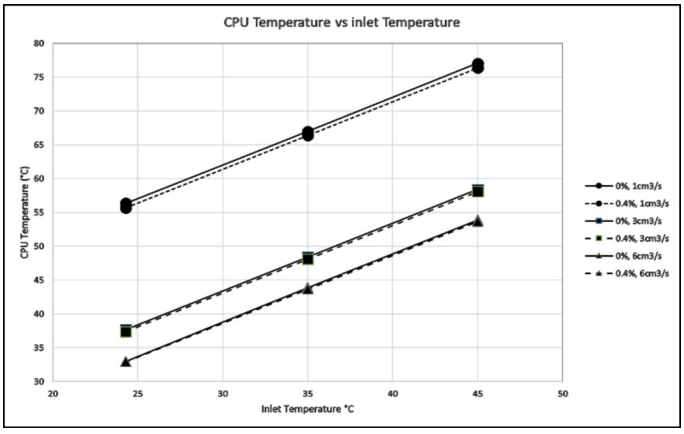

FIGURE 10: EFFECT OF VOLUMETRIC CONCENTRATION OF NANOPARTICLES ON CPU TEMPERATURE FOR DIFFERENT COOLANT INLET TEMPERATURES

The heat transfer in this case is based on convection. For a high velocity, the gradient of temperature close to the walls becomes very high. Therefore, it is difficult to detect the effect of increase in thermal conductivity. Therefore, when the flow rate is increased to $3cm^3/s$ and $6cm^3/s$, the temperature remains constant. The value of Nusselt number was calculated based on the flow Reynolds and Prandtl Number using a relation from published literature as shown in equation 8. The fraction for wall viscosity and nanofluid viscosity in equation 8 is assumed to be equal to unity as no spatial variation of viscosity is considered. [39]. A reduction of 0.5-1% was observed in the absolute value of Nusselt Number for each of the particle concentration. This reduction does not necessarily depict a reduction in heat transfer. It has been established in the reviewed literature that this reduction might be attributed to a difference in increase of thermal conductivity and heat transfer coefficient. This can be verified from the fact that the convective heat transfer coefficient, h, is directly proportional to approximately $Re^{1/3}$ and $Pr^{1/3}$ for laminar flows. Thus, the Nusselt Number reduces proportional by a same degree. This reduction in Nusselt number is usually the least for water and increases for other some fluids like ethylene glycol.

$$\overline{Nu_{nf_{th}}} = 1.86\left(Re_{nf}.Pr_{nf}.\frac{D}{L}\right)^{\frac{1}{3}}\left(\frac{\mu_{nf}}{\mu_{nf}}\right)^{0.14} \quad (8)$$

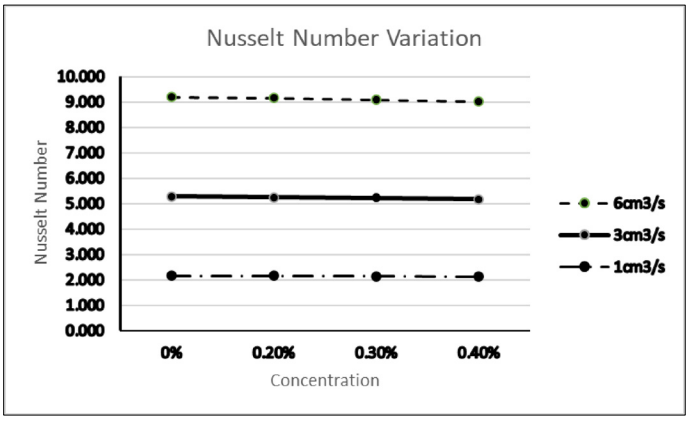

FIGURE 11: VARIATION OF NUSSELT NUMBER WITH PARTICLE CONCENTRATION

Figure 12 shows the variation of Nusselt number vs Reynolds number. While some studies report the increase in Nusselt number with increasing particle concentration, but there are a few experimental studies which state otherwise as well. The trend obtained for all the concentrations in the present investigation is similar to that in published literature where the Nusselt number for any given concentration increases with the Reynolds number, implying that there is an increase in the convective heat transfer due to enhancement of heat transfer properties when compared to the base fluid. The change in the Nusselt number is not significant as the concentrations considered in the present investigation do not vary a lot and the variation of the Prandtl number is also not significant, a minimum of 5.7 to a maximum of 6.3 in this case.

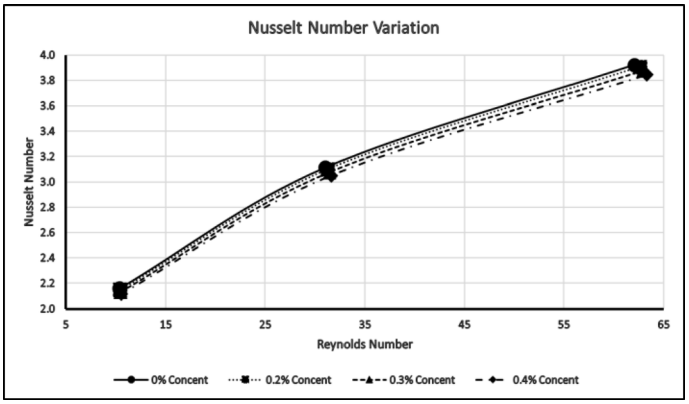

FIGURE 12: VARIATION OF NUSSELT NUMBER VS REYNOLDS NUMBER

The enhancement in the convective heat transfer process can be seen by analyzing the change in the convective heat transfer coefficient value. A maximum variation of approximately 10% was observed for the case for maximum flowrate at 0.4% particle concentration. This is a significant enhancement in the overall heat transfer process. The same value increased by 8.5% and 7.95% in case of 0.3% and 0.2% particle concentration, respectively.

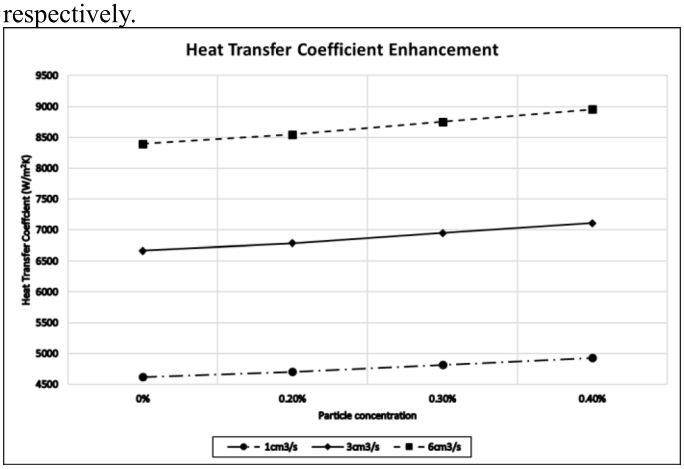

FIGURE 13: VARIATION OF CONVECTIVE HEAT TRANSFER COEFFICIENT WITH PARTICLE CONCENTRATION

Figures 14 and 15 represent the temperature contours at the walls of the channel for flow at 6cm3/s and a nanoparticle concentration of 0% and 0.3% respectively. The coolant enters the system from the inlet on the left, flows through the microchannels and exits through the outlet on the top side of the geometry. This varying contour shape appears because the current cold plate is an impingement type cold plate which causes more cooling at the center where the flow impinges on the center partition of the fins. The streamline plot of the flow velocity was not included in the manuscript to avoid repetition. But it shows significant flow separation towards the outlet which causes higher temperature near the outlet.

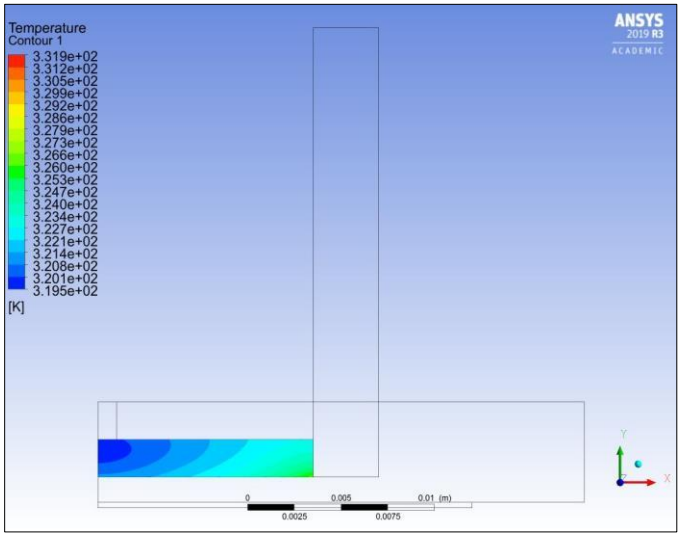

FIGURE 14: TEMPERATURE CONTOURS FOR 6CM^3/S FLOW RATE AND 0.3% CONCENTRATION

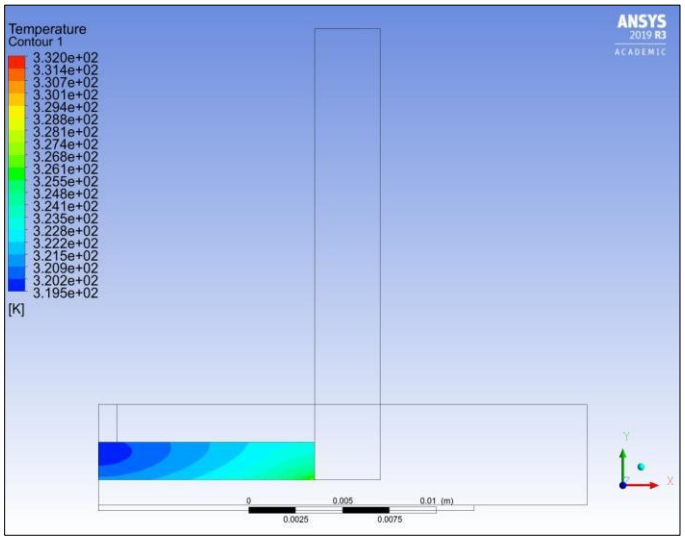

FIGURE 15: TEMPERATURE CONTOURS FOR 6CM^3/S FLOW RATE AND 0% CONCENTRATION

CONCLUSION AND FUTURE WORK

According to the observations of the results, when the concentration of the nanoparticles increases more than 3%, the temperature drop with respect to the pressure drop is not very high. Thus, we can conclude that a 3% concentration of copper nanoparticles in a base fluid of water is optimal. To have a better understanding of the nanofluid, simulations need to be performed with lower flow rates and higher inlet temperature, because at a lower inlet flow, the heat transfer to the fluid is higher and at higher temperatures. To further reduce the pressure-drop across the system, the geometry of the cold plate can be optimized. Also, on the base of cold plate temperature, an

automated flow control valve can be used to control the mass flow rate. This will further reduce the overall cost of each server and in turn, the data centers. The concerns pertaining to particle sedimentation and agglomeration have also been addressed in the literature which suggest that addition of stabilizing agents and surfactants can prevent the afore-mentioned phenomenon. The sedimentation is usually balanced by the dominant Brownian Forces but increases with increasing agglomeration which can be addressed during the nanofluid preparation [50].

The issue of contamination related failures limit cost effective air-cooling techniques to be successfully implemented for data centers looking to lower their PUE. While it's true that air cooling will continue to dominate the data center cooling industry, especially for enterprise storage systems, and latest phase change and direct immersion cooling techniques are also being used for cooling high performance clusters, indirect liquid cooling presents the simplest and the best option for cooling high heat fluxes without significant changes to existing data center infrastructure [40-48]. As the current study indicates, thermal enhancements like improvement of heat transfer characteristics of the coolant can further aid in better and efficient cooling of high-performance servers. Future studies by the authors on this topic will focus on validating the implementation of nanofluid coolants at rack level using simulations so that the performance enhancement at data center level can be measured. The performance of this cold plate will also be validated using multiphase simulation to assess the exchange terms between two phases of the nanofluid and the results can be compared with those obtained from present simulation. Multiphase simulations will aid in assessment of the regions of particle aggregation and investigation of the effect of dispersed phase behavior within the base fluid on other hydrodynamic characteristics.

REFERENCES

[1] Arman Shehabi, Sarah Josephine Smith https://eta.lbl.gov/publications/united-states-data-center-energy

[2] Yaser Hadad*, Reza Pejman, "Geometric Optimization of an Impinging Cold-Plate with a Trapezoidal Groove Used for Warm Water Cooling" 17th IEEE ITHERM Conference

[3] Tonapi, S. S., Fillion, R. A., Schattenmann, F. J., Cole, H. S., Evans, J. D., and Sammakia, B. G., 2003, "An Overview of Thermal Management for Next Generation Microelectronic Devices," Advanced Semiconductor Manufacturing Conference and Workshop, IEEEI/SEMI (ASMC), Munich, Germany, Mar. 31–Apr. 1, pp. 250–254.

[4] Chu, R. C., Bar-Cohen, A., Edwards, D., Herrlin, M., Price, D., Schmidt, R., and Sammakia, B., 2003, "Thermal Management Roadmap Cooling Electronic Products From Handheld Device to Supercomputers," MIT Rohsenow Symposium, Cambridge, MA, May 16.

[5] Alkharabsheh, S., Fernandes, J., Gebrehiwot, B.,Agonafer, D., Ghose, K., Ortega, A., Joshi, Y., and Sammakia, B., 2015, "A Brief Overview of Recent Developments in Thermal Management in Data Centers," ASME. J. Electron. Packag., 137(4), p. 040801.

[6] Ellsworth, M. J., Jr., and Iyengar, M. K., 2009, "Energy Efficiency Analyses and Comparison of Air and Water Cooled High Performance Servers," ASME Paper No. InterPACK2009-89248.

[7] David, M., Iyengar, M., Parida, P., Simons, R., Schultz, M., Gaynes, M., Schmidt, R., and Chainer, T., 2012, "Experimental Characterization of an Energy Efficient Chiller-Less Data Center Test Facility With Warm Water Cooled Servers," 28th Annual IEEE Semiconductor Thermal Measurement and Management Symposium (SEMI-THERM), San Jose, CA, Mar. 18–22, pp. 232–237.

[8] Bharath Ramakrishnan, Yaser Hadad *"Thermal Analysis of Cold Plate for Direct Liquid Cooling of High Performance Servers" ASME Journal 041005-6 / Vol. 141, DECEMBER 2019*

[9] A. E. Bergles, Survey and Evaluation of Techniques to Augment Convective Heat and Mass Transfer, in U. Grigull and E. Hahne (eds.), *Progress in Heat and Mass Transfer* vol. 1, pp. 331-424, Pergamon Press, New York, 1969.

[10] W. Nakayama, Enhancement of Heat Transfer, *Heat Transfer 1982, Proc. 7th Int. Heat Transfer Conf.,* vol. 1, pp. 223-240, Hemisphere, Washington, DC, 1982.

[11] A. E. Bergles, Some Perspectives on Enhanced Heat Transfer-Second-Generation Heat Transfer Technology, *Trans. ASME, J. Heat Transfer,* vol. 110, pp. 1082-1096, 1988.

[12] A. E. Bergles, Augmentation of Heat Transfer, in *Heat Exchanges Design Handbook,* vol. 2, pp. 2.5.11-1-12, Hemisphere, Washington, DC, 1983.

[13] A. E. Bergles, Techniques to Augment Heat Transfer, in *Handbook of Heat Transfer Applications,* pp. 3-1-80, McGraw-Hill, New York, 1985

[14] Pak, Bock Choon, and Young I. Cho. "Hydrodynamic and heat transfer study of dispersed fluids with submicron metallic oxide particles." *Experimental Heat Transfer an International Journal* 11.2 (1998): 151-170.

[15] Chein, Reiyu, and Jason Chuang. "Experimental microchannel heat sink performance studies using nanofluids." *International journal of thermal sciences* 46.1 (2007): 57-66.

[16] D.B. Tuckerman, R.F. Pease, High-performance heat sinking for VLSI, IEEE Electronic Devices Letters, EDL 2 (1981) 126–129.

[17] H.Y. Wu, P. Cheng, An experimental study of convective heat transfer in silicon microchannels with different surface conditions, Int. J. Mass Heat Transfer 46 (2003) 2547–2556.

[18] W. Qu, I. Mudawar, Experimental and numerical study of pressure drop and heat transfer in a single-phase micro-channel heat sink, Int. J. Heat Mass Transfer 45 (2002) 2549–2565.

[19] R.W. Knight, D.J. Hall, J.S. Goodling, R.C. Jaeger, Heat sink optimization with application to microchannels, IEEE Transactions on Components, Hybrids, and Manufacturing Technology 15 (1992) 832–842.

[20] A. Horvat, I. Catton, Numerical technique for modeling conjugate heat transfer in an electronic device heat sink, Int. J. Heat Mass Transfer 46 (2003) 2155–2168.

[21] K.V. Liu, S.U.S. Choi, K.E. Kasza, Measurements of pressure drop and heat transfer in turbulent pipe flows of particulate slurries, Report, Argonne National Laboratory, 1988, ANL-88-15.
[22] R.L. Webb, Principles of Enhanced Heat Transfer, John Wiley & Sons, New York, 1993.
[23] X. Wang, X. Xu, S.U.S. Choi, Thermal conductivity of nanoparticle-fluid mixture, J. Thermophys. Heat Transfer 13 (1999) 474–480.
[24] S. Lee, S.U.S. Choi, S. Li, J.A. Eastman, Measuring thermal conductivity of fluids containing oxide nanoparticles, J. Heat Transfer 121 (1999) 280–289.
[25] B.X.Wang, L.P. Zhou, X.F. Peng, A fractal model for predicting the effective thermal conductivity of liquid with suspension of nanoparticles, Int. J. Heat Mass Transfer 46 (2003) 2665–2672.
[26] J. Koo, C. Kleinstreuer, A new thermal conductivity model for nanofluids, J. Nanoparticle Research 6 (2004) 577–588.
[27] Y. Xuan, W. Roetzel, Conceptions for heat transfer correlation of nanofluids, Int. J. Heat Mass Transfer 43 (2000) 3701–3707.
[28] Q. Li, Y. Xuan, Convective heat transfer and flow characteristics of Cu–water nanofluid, Science in China, Series E 45 (2002) 408–416.
[29] Y. Xuan, Q. Li, Investigation on convective heat transfer and flow features of nanofluids, ASME J. Heat Transfer 125 (2003) 151–155.
[30] B.C. Pak, Y.L. Cho, Hydrodynamic and heat transfer study of dispersed fluids with submicron metallic oxide particles, Exp. Heat Transfer 11 (1998) 151–170.
[31] Y. Yang, Z. Zhang, E.A. Grulke, W.B. Anderson, Heat transfer properties of nanoparticle-influid dispersions (nanofluids) in laminar flow, Int. J.Heat Mass Transfer 48 (2005) 1107–1116.
[32] J. Koo, C. Kleinstreuer, Laminar nanofluid flow in microheat-sinks, Int. J.Heat Mass Transfer 48 (2005) 2652–2661.
[33] R. Chein, G. Hunag, Analysis of microchannel heat sink performance using nanofluids, Applied Thermal Engineering 25 (2005) 3104–3114.
[34] *ANSYS® ANSYS CFX-Solver Theory Guide, Chapter 1, Release 2019 R3*
[35] Purohit, N.; Purohit, V.A.; Purohit, K. Assessment of nanofluids for laminar convective heat transfer: A numerical study. Eng. Sci. Technol. Int. J. 2016, 19, 574–586
[36] Das, S.K.; Putra, N.; Thiesen, P.; Roeztzel, W. Temperature dependence of thermal conductivity enhancement for nanofluids. J. Heat Transf. 2003, 125, 567–574
[37] Wang, X.Q.; Mujumdar, A.S. A review on nanofluids—Part I: Theoretical and numerical investigations. Braz. J. Chem. Eng. 2008, 25, 613–630
[38] Brinkman, H.C. The viscosity of concentrated suspensions and solutions. J. Chem. Phys. 1952, 20, 571
[39] Seider, E.N., Tate, G.E., 1936. Heat transfer and pressure drop of liquid in tubes. Industrial Engineering Chemistry 28 (12), 1429–1435
[40] Jimil M. Shah, Chinmay Bhatt, Pranavi Rachamreddy, Ravya Dandamudi, Satyam Saini, Dereje Agonafer, 2019, Computational Form Factor Study of a 3rd Generation Open Compute Server for Single-Phase Immersion Cooling, ASME Conference Paper No. IPACK2019-6602
[41] Dhruvkumar Gandhi, Uschas Chowdhury, Tushar Chauhan, Pratik Bansode, Satyam Saini, Jimil M. Shah and Dereje Agonafer, 2019, Computational analysis for thermal optimization of server for single phase immersion cooling, ASME Conference Paper No. IPACK2019-6587
[42] Pravin A Shinde, Pratik V Bansode, Satyam Saini, Rajesh Kasukurthy, Tushar Chauhan, Jimil M Shah and Dereje Agonafer, 2019, Experimental analysis for optimization of thermal performance of a server in single phase immersion cooling, ASME Conference Paper No. IPACK2019-6590
[43] Jimil M. Shah, Roshan Anand, Satyam Saini, Rawhan Cyriac, Dereje Agonafer, Prabjit Singh, Mike Kaler, 2019, Development of A Technique to Measure Deliquescent Relative Humidity of Particulate Contaminants and Determination of the Operating Relative Humidity of a Data Center, ASME Conference Paper No. IPACK2019-6601
[44]Gautham Thirunavakkarasu, Satyam Saini, Jimil Shah, Dereje Agonafer,2018, Airflow pattern and path flow simulation of airborne particulate contaminants in a high-density Data Center utilizing Airside Economization, ASME Conference Paper No. IPACK2018-8436
[45] Kumar, A., Shahi, P., & Saha, S. K. Experimental Study of Latent Heat Thermal Energy Storage System for Medium Temperature Solar Applications.
[46] Saini, Satyam. Airflow Path and Flow Pattern Analysis of Sub-Micron Particulate Contaminants in a Data Center with Hot Aisle Containment System Utilizing Direct Air Cooling. Diss. 2018.
[47] Dehkordi, B. G., Fallah, S., & Niazmand, A. (2014). Investigation of harmonic instability of laminar fluid flow past 2D rectangular cross sections with 0.5–4 aspect ratios. Proceedings of the Institution of Mechanical Engineers, Part C: Journal of Mechanical Engineering Science, 228(5), 828–839. https://doi.org/10.1177/0954406213491906
[48] Shahi, Pardeep, 2016, “Experimental Analysis of PCM based Thermal Storage System for Solar Power Plant,” M.S. thesis, Indian Institute of Technology- Mumbai.
[49] CoolITSystems, “CoolITSystemsManual,” accessed January 30th, 2019, https://www.coolitsystems.com/passive-coldplate-loop/
[50] Ilyas, Suhaib Umer, Rajashekhar Pendyala, and Narahari Marneni. "Preparation, sedimentation, and agglomeration of nanofluids." *Chemical Engineering & Technology* 37, no. 12 (2014): 2011-2021.